GFZ

Helmholtz-Zentrum
POTSDAM

HELMHOLTZ-ZENTRUM POTSDAM
DEUTSCHES
GEOFORSCHUNGSZENTRUM

Robert Dill

Hydrological model LSDM for operational Earth rotation and gravity field variations

Scientific Technical Report STR08/09

www.gfz-potsdam.de

HELMHOLTZ
GEMEINSCHAFT

Hydrological model LSDM for operational Earth rotation and gravity field variations

Robert Dill
Section 1.5: Earth System Modelling
Helmholtz Centre Potsdam
GFZ German Research Centre For Geosciences
Public Law Foundation State of Brandenburg
Telegrafenberg, D-14473 Potsdam, Germany.
E-mail: dill@gfz-potsdam.de

ABSTRACT

Water mass redistributions within the global hydrological cycle are one of the main endogenous geophysical processes causing Earth rotation and gravity field variations on seasonal to inter-annual time scales. To simulate hydrospheric induced Earth orientation parameters and gravity field coefficients the complex system of global water mass transports has to be modelled. Operational data of atmospheric and oceanic water mass redistributions are widely used for near real-time simulations of hydrospheric Earth rotation excitation and gravity field representations. They are also essential for de-aliasing purposes of the GRACE (Gravity Recovery Climate Experiment) gravity products. In addition to atmosphere and ocean, seasonal and inter-annual variations are caused by continental water mass redistributions. In order to account for the terrestrial hydrology processes as well and to close the global water cycle, continental water mass storage fields and fluxes are needed in the same operational manner as for atmosphere and ocean. The operational LSDM (Hydrological Land Surface Discharge Model), presented here, has been built on the basis of the existing SLS (Simplified Land surface Scheme) and HDM (Hydrological Discharge Model). These two sub-models have been recoded, extended, and combined to enable a consistent operational simulation of continental water mass redistributions in the focus of a global hydrosphere simulation system. The processing system of LSDM, including the new land surface module LSXM (Land Surface eXtended Model), the revised discharge module HDXM (Hydrological Discharge eXtended Model), and optimized mass conservative remapping algorithms, has been adjusted to work closely with ECMWF (European Centre for Medium-Range Weather Forecasts) atmospheric forcing fields. Alternative atmospheric forcing from other models like NCEP (National Centers for Environmental Prediction) or the climate model ECHAM can be easily implemented in the same fashion. LSDM routinely provides

DOI: 11.2312/GFZ.b103-08095

in near real-time daily variations of global water mass storage and corresponding water mass fluxes, as well as hydrological angular momentum (HAM) functions and low degree gravity field coefficients. In combination with the operational ocean model OMCT (Ocean Model for Circulation and Tides), also forced by ECMWF data, the complete set of atmospheric, oceanic, and hydrological mass variations allows a realistic and consistently closed representation of mass transports in the hydrological cycle.

TABLE OF CONTENTS

1 Introduction 5
2 LSDM hydrological modelling 7
2.1 Land surface module LSXM 9
2.2 Discharge module HDXM 13
2.3 Mass conservative remapping 18
2.4 Implementation of an operational hydrological processing scheme 20
2.5 Indirect hydrological effect 21
3 Validation of simulated continental discharge 23
4 Validation of the continental hydrological budget 25
5 Hydrological angular momentum, HAM 26
6 Comparison of simulated and observed C_{20} gravity coefficients . . . 29
7 Conclusions 32
REFERENCES 33

DOI: 11.2312/GFZ.b103-08095

1 INTRODUCTION

Within the global hydrological cycle the terrestrial hydrology covers all water transport processes over land, routing the atmospheric rainfall to the oceans. Continental hydrology represents the water distribution in rivers and lakes, groundwater storage, soil moisture and water accumulated as snow and ice, as well as water contents in the biosphere. The continental freshwater accounts only for 3.5% of the total global water masses which are concentrated in the oceans. More than one half of this freshwater is combined as ice, glacier or permafrost and almost all of the rest is groundwater. Nevertheless, the redistribution and retention mechanisms of the residual 0.2 Mio m^3 water in rivers and lakes affect significantly global geodetic Earth parameters, such as Earth rotation, the Earth's shape, and its gravity field, especially on seasonal to inter-annual time scales. Knowledge of continental water storage and freshwater runoff into the oceans is also essential for the reliable representation of consistent physical fluxes among the atmosphere, the oceans, and continental hydrosphere. In the focus of a dynamically coupled global climate system, continental hydrology and the accurate description of inter-model mass exchanges are mandatory. Furthermore, global water redistributions are required for de-aliasing purposes within the GRACE (Gravity Recovery Climate Experiment) satellite mission. The main influences, arising from atmosphere and oceans, are nowadays modelled routinely in near real-time. In contrast, most continental hydrology models operate as annual stand-alone re-analysis programs controlled by a complex set of input parameters not available in real-time. This causes an unacceptable delay up to more than one year. In consequence the combination of atmospheric, oceanic, and hydrological model results yields not necessarily a closed water balance. To account for hydrological processes in the same operational manner as for atmosphere and oceans, an operational hydrological processing scheme, filling the land surface gap in the hydrological cycle, has been developed.

For the operational near real-time simulation system LSDM (Land Surface Discharge Model) the Hydrological Discharge Model (HDM) from the Max-Planck-Institute for Meteorology (MPI-M) in Hamburg (Hagemann & Dümenil, 1998a), combined with the Simplified Land Surface scheme (SLS) (Hagemann & Dümenil, 2003), offered the most suitable starting basis. In the framework of two project packages founded by the German Research Foundation (DFG), "Earth System Model" and "Earth rotation and the ocean's circulation", HDM and SLS have already been used and tested extensively. As hydrological component HDM has been embedded in a coupled modelling system together with an atmospheric component from the climate model ECHAM or the weather model ECMWF (European Centre for Medium-Range Weather Forecasts), and an oceanic component from OMCT (Ocean Model for Circulation and Tides) or LSG (Large Scale Geostrophic model) (Sündermann et. al, 2008). Both DFG projects emphasized the ability of HDM, combined with SLS, to reproduce reliable continental water mass distributions. The initial HDM sub-model has already been extended by subroutines to calculate global geodetic parameters, such as hydrological induced Earth rotation variations. With a variety of atmospheric forcing conditions the impact of hydrological mass redistributions on Earth rotation parameters and gravity field coefficients has been estimated (Walter, 2008). Furthermore, the detailed analyses of hydrological

DOI: 11.2312/GFZ.b103-08095

angular momentum (HAM) functions from the combination of the initial stand-alone versions of SLS and HDM pointed out that the handling of water fluxes among different models in a conservative way is crucial for reliable estimations of global geodetic parameters. This task includes the water mass exchanges among atmosphere, continental hydrosphere, and oceans as well as the internal exchange among the land surface module SLS and the discharge module HDM. The positive experience and expertise gained within the DFG projects motivated for further investigations to close the gap between atmospheric models and ocean circulation models in the global water cycle more consistently than this had been achieved so far.

To satisfy the requirements of operationality and consistency, several extensions and innovations to the existing SLS and HDM were necessary. The model LSDM embeds the new set of land surface module LSXM (Land Surface eXtended Model) and discharge module HDXM (Hydrological Discharge eXtended Model) in specific pre- and post-processing routines to ensures not only model internal consistency, but also external balanced mass exchanges with atmospheric and oceanic models. The to date routinely operating processing system LSDM has been designed for the coupling with atmospheric and oceanic models, both forced by ECMWF data. However, the modelling system could easily be adapted to NCEP (National Centers for Environmental Prediction) data, for example, as well.

This technical scientific report introduces in chapter 2 the applied hydrological modelling approach and summarizes the accomplished improvements for the LSXM module in chapter 2.1 and the HDXM module in chapter 2.2. In combination with a mass conservative remapping, chapter 2.3, and an operational processing scheme, chapter 2.4, the LSDM offers a fully operational hydrological simulation system.

model	description	author
SLS + HDM	original stand-alone versions, F77 code from MPI, Hamburg. (unequal land-ocean representation)	Hagemann and Dümenil, 1998
SLS + HDM + HAM calculation	same HDM also used in ECOCTH model - calculation of hydrol. ang. momentum HAM - 3-D topography for HAM - spherical harmonic expansion for gravity field - misaligned land-ocean parts excluded	model 1) for comparison Walter, 2007
LSXM + HDXM	recoded in fast and stable F90 - adjusted land-ocean mask - rigorous field initialisation - incorporate glaciated regions - low degree gravity coefficients - lake/swamp reformulation	Dill, 2007
LSDM operational	fully automatic processing scheme, results available via FTP - operational pre- and postprocessing - enhanced estimation of evaporation - mass-conservative remapping	model 2) for comparison Dill, 2008
LSDM operational using ext. evaporation	read evaporation estimates from atmospheric land surface model, here ECMWF (TESSEL)	model 3) this report ftp.gfz-potsdam.de →public/ig/dill

Table 1. History of hydrological model development.

The operational daily output of HAM time series and low degree gravity coefficients as well as consistently reprocessed results for the period 1958-2000 covered by ECMWF's re-analyses project ERA-40 are publicly available for the scientific community (see FTP access later on). Chapter 2.5 introduces the handling of the indirect hydrological effect, also provided per FTP. The history of model developments is listed in table 1. Results from three model stages, named model 1) - 3), have been analysed and compared to check the influence and improvement of each single alteration step. The LSDM model has been validated by comparing analyses of simulated and observed river discharge rates as presented in chapter 3. The continental hydrological budget has been checked to ensure mass conservation (chapter 4). Finally, the seasonal signal of the generated HAM time series and low degree gravity field coefficients are presented in chapter 5 and 6, respectively.

2 LSDM HYDROLOGICAL MODELLING

Continental water storage summarizes surface water in rivers, lakes, wetlands and reservoirs, groundwater and soil moisture, as well as water accumulated as snow and ice. Water contents in the biosphere like water in and on vegetation and human water consumption belong to hydrology, too. Direct observations of the total water storage are often restricted to point measurements of single components, although since a few years a new type of information about the spatial and temporal variations of continental water storage on a global scale is available from the GRACE satellite mission. Indirect estimations can be obtained by solving the continental water balance (equation 1). Changes of the total water storage, W, can be described generally as difference between incoming precipitation, P, and the outcome represented as evaporation, E, and discharge into the oceans, Q, i.e.,

$$\Delta W = P - E - Q. \tag{1}$$

Assigning the global budget described by equation 1 to local catchments or model grid cells and distinguishing for the discharge between surface runoff, R, and groundwater drainage, D, with $Q = R + D$ the local water balance yields

$$\Delta W_{loc} = P_{loc} - E_{loc} - R_{loc} - D_{loc} + Q_{in} - Q_{out} \tag{2}$$

Equation 2 can be divided into the vertical water balance

$$\Delta W_{loc}^{vert} = P_{loc} - E_{loc} - R_{loc} - D_{loc} \tag{3}$$

accounting for water mass variations stored in soil moisture, snowpacks, and ice, and the lateral water balance

$$\Delta W_{loc}^{lat} = Q_{in} - Q_{out} \tag{4}$$

considering the horizontal water mass transports among grid cells. Precipitation P is one of the main output parameters of global weather forecast systems and represents the only water mass input for the continental hydrology system. Evaporation E is estimated by a land surface model (LSM) either included in the atmospheric

DOI: 11.2312/GFZ.b103-08095

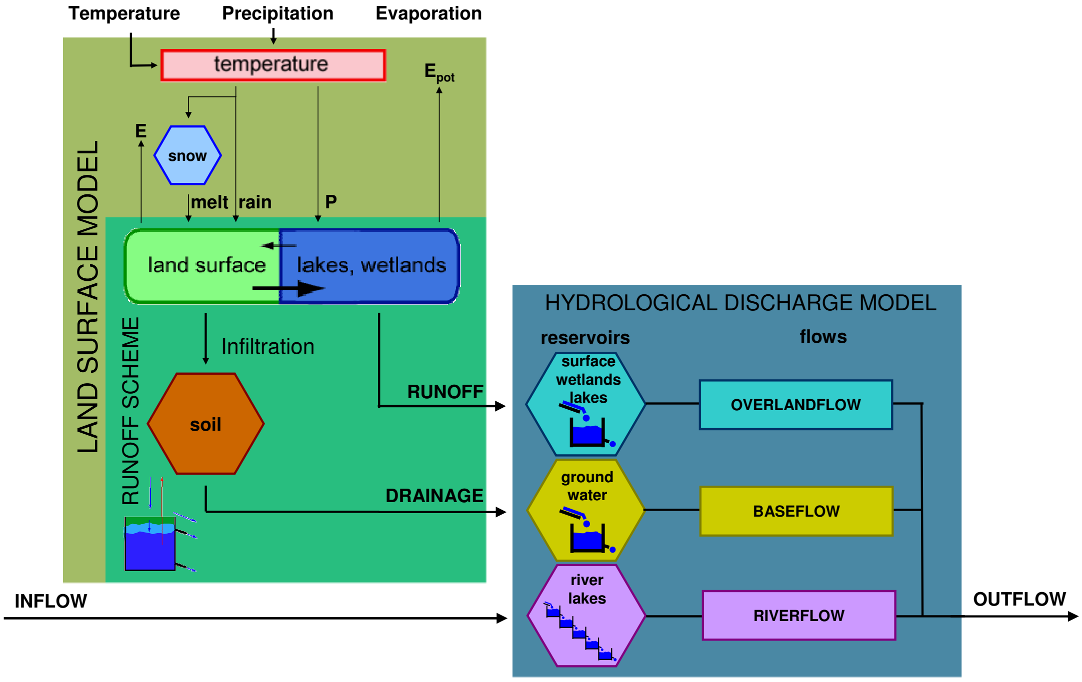

Figure 1. Continental hydrological modelling: Combination of the land surface module LSXM with the hydrological discharge module HDXM via runoff and drainage.

model or treated separately with an additional LSM module. The realistic modelling of evaporation rates is crucial for a consistent atmosphere-land coupling. Runoff R and drainage D are the two other output fluxes generated by the LSM. They connect the vertical and the lateral water balance. Runoff and drainage refill the lateral flow reservoirs. The incoming water fluxes Q_{in} arise out of river flow, runoff, and drainage of upstream regions. Q_{out} summarizes all outflows routed by the river-network downstream. Similar to the vertical and lateral water balance the hydrological model can be divided into two modules in series. The lateral water flow processes are described by the discharge module HDXM (see section 2.2). It requires external input data separated into runoff and drainage, contributing to the internal overland flow and base flow respectively (Fig. 1). Unlike the atmospheric climate model ECHAM, the land surface schemes of the weather models ECMWF and NCEP and corresponding re-analysis data do not directly provide these forcing data sets appropriate to HDXM. Therefore, a second module, describing the land surface processes separately, has to precede the HDXM. The land surface module LSXM (see section 2.1) separates the incoming precipitation rates from the atmosphere into snow accumulation and water infiltrating the soil according to the actual temperature, provided by the atmospheric model, and the internal defined soil capacity distributions. It generates surface runoff, groundwater drainage and evaporation back to the atmosphere (Fig. 1).

The impact of terrestrial water mass redistributions on global geodetic parameters can be derived by integrating globally over all continental water masses. The vertical water balance is estimated either from the sum of soil moisture and snow

DOI: 11.2312/GFZ.b103-08095

contents in the land surface module

$$W^{vert} = W^{soil} + W^{snow} \tag{5}$$

or indirectly via the vertical flux budget (equation 3). The lateral water balance summarizes all water in flow reservoirs such as swamps, lakes, rivers and groundwater and needs the exact spatial water distribution in all flow reservoirs.

$$W^{lat} = \sum W^{reservoirs} \tag{6}$$

The knowledge of the varying water masses in the lateral flows in combination with the lateral flow distances allows also estimates of the dynamic influence on Earth rotation via relative angular momentum exchanges (see section 5).

2.1 Land surface module LSXM

The Land Surface eXtended Model LSXM is based on the Simplified Land Surface scheme SLS (Hagemann & Dümenil, 2003). It is optimized for the concatenation of ECMWF atmospheric data with the discharge module HDXM.

The original SLS module refers to the land surface parametrization of the atmospheric climate model ECHAM4, interpolated to a global 0.5° x 0.5° grid. For each grid cell LSXM processes the incoming precipitation through the following sequence of subroutines, described below in detail:

- precipitation form: devide precipitation into rain or snow, according to temperature
- snowmelt: meltwater from snowpack according to temperature degree-day approach
- rainmelt: snowmelt caused by rain onto snowpack
- refreezing: gradually refreezing of fluid water content in snowpack
- throughfall: sum of rain - snow + snowmelt
- excess runoff: fast surface runoff using Arno scheme with local water capacities
- drainage: water percolating into the deeper soil using local water storage content
- potential evaporation: according to Thornwaite method using T from atmospheric model
- actual evaporation: estimating E using pot. E, skin water, and vegetation characteristics
- lakes and swamps: special adjustment of retention times in wet areas

2.1.1 Basic SLS

Within each grid cell precipitation is separated into rain and snow depending on a temperature model according to Wigmosta et al. (1994). Below -1.1°C, precipitation falls as snow and is accumulated to the snowpack. Between -1.1°C and +3.3°C precipitation fades linearly from snow to rain. Above 3.3°C precipitation falls as pure rain.

Snowmelt is estimated with a degree-day factor approach assuming that melt rates are linearly related to the air temperature, as in the HBV model (Hydrologiska Byråns Vattenbalansavdelning), (Bergstroem, 1992), from the Hydrological Bureau Waterbalance-section at the Swedish Meteorological and Hydrological Institute (SMHI). Melt water runoff is delayed by the water holding capacity of snow. Retaining rain or melt water in the snowpack is allowed to refreeze gradually when temperature decreases below 0°C. Leaking melt water and rain is then merged as throughfall reaching the soil surface.

Throughfall is separated into surface runoff (fast runoff) and water that may

DOI: 11.2312/GFZ.b103-08095

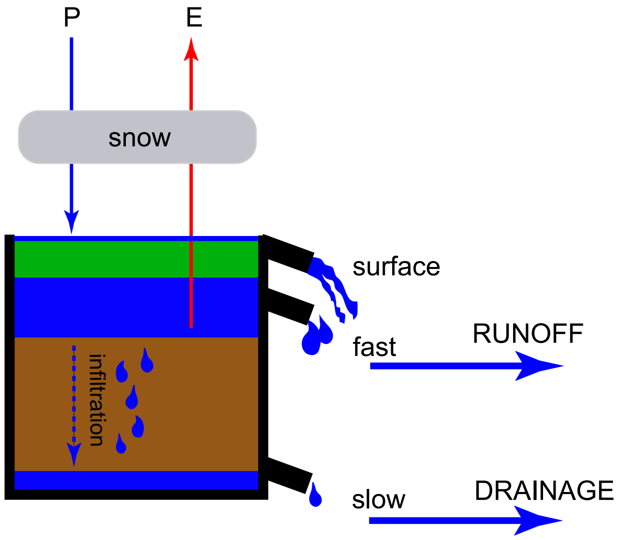

Figure 2. Runoff scheme: Bucket scheme separating throughfall into runoff, infiltration, and drainage.

infiltrate into the soil by an improved Arno scheme (Dümenil & Todini, 1992; Hagemann & Dümenil, 2003). Drainage (slow runoff) is a small amount of water that is allowed to leave the soil downwards. Each grid cell is described by a bucket-like soil reservoir (Fig. 2). Originally, the bucket scheme represented no horizontal heterogeneities of the soil within a grid cell. The improved Arno scheme accounts for the sub-grid variability of soil saturation within a grid cell. Instead of the statistical distribution of sub-grid scale soil water capacities like in the former Arno scheme, the improved parametrization uses individual fractional saturation curves, derived from high resolution soil water capacity data sets. The saturation curves are determined by three optimized parameters. w_{min} is the minimum local soil water capacity. The grid cell soil can be filled up with water until the maximum local soil capacity w_{max}. The shape of the curve is defined by parameter b reflecting the topographic variability within one grid cell. b depends on the model resolution. Between the boundaries w_{min} and w_{max} the actual sub-grid water content w_{act}, that corresponds to the fractional saturation of s/S of the grid cell, is given by

$$\frac{s}{S} = 1 - \left(\frac{w_{max} - w_{act}}{w_{max} - w_{min}}\right)^b \tag{7}$$

where s/S is the percentage of the grid cell area S that is saturated. The parameter b is defined as

$$b = max\left[\frac{\sigma_h - \sigma_0}{\sigma_h + \sigma_{max}}; 0.01\right] \tag{8}$$

Here σ_h is the standard deviation of orography within a model grid cell calculated from the 30-arc-second topography dataset GTOPO30 (Bliss & Olsen, 1996). σ_0 and σ_{max} are the minimum and maximum standard deviations of orography at the grid resolution, respectively. Only in mountainous regions b differs significantly from 0.01. This approach accounts for two expectations. First, more than aver-

DOI: 11.2312/GFZ.b103-08095

age runoff is produced in mountainous regions, and second, in steep terrain the probability that soil water capacities in the lower parts within a grid cell reach saturation is higher than for flat terrain due to small scale hillslope flow processes.

Within a grid cell the soil water content can reach locally (sub-grid) w_{act}, but can be smaller as well. The actual soil water content W^{soil} of the whole grid cell can be derived from equation 7 and 8 by

$$W^{soil} = w_{min} + \int_{w_{min}}^{w_{act}} (1 - \frac{s}{S}) dw \qquad (9)$$

When a rainfall event rises the actual water storage capacity to w_{act}, equation 9 expresses the amount of water W^{soil} which can be stored in the soil. The rest of the total throughfall, not infiltrated into the soil, will generate surface runoff. In contrast to the simple bucket scheme, runoff may occur even if the whole grid cell is not yet saturated (Fig. 3). In addition to the runoff remaining on the surface, drainage is the amount of water that percolates downwards from the bucket into the deeper soil.

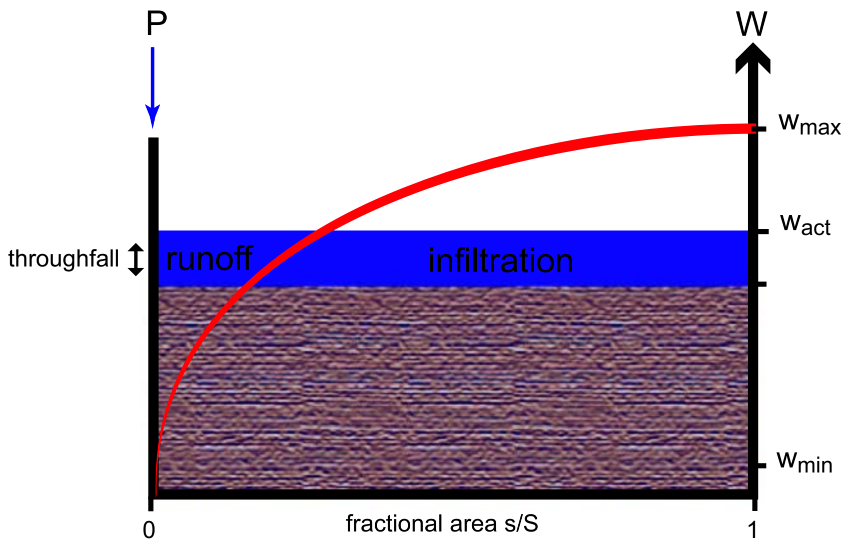

Figure 3. Improved Arno scheme (Hagemann & Dümenil, 2003).

The third outcoming flux, calculated from the land surface module, is evaporation. Actual evaporation can be expressed as a function of potential evaporation estimates. It is the sum of baresoil evaporation using soil moisture storage and capacities, and transpiration using seasonal vegetation and wilting point indices (Roeckner et. al, 1992). Over wetlands and lakes the actual evaporation is raised to the potential evaporation level. Potential evaporation is computed according to the Thornthwaite formula (Chebotarev, 1977) from annual mean temperature

DOI: 11.2312/GFZ.b103-08095

characteristics.

$$\mathrm{pot}E_i = \begin{cases} 0 & T < 0°\mathrm{C} \\ 16\left(\frac{10T_i}{I}\right)^a & 0 \le T \le 26.5°\mathrm{C} \\ -415.85 + 32.24T_i - 0.43T_i^2 & T \ge 26.5°\mathrm{C} \end{cases} \tag{10}$$

T indicates the mean surface air temperature in month i in °C. The exponent a is empirically defined as

$$a = \left(0.675 \cdot I^3 - 77.1 \cdot I^2 + 17920 \cdot I + 492390\right) \cdot 10^{-6} \tag{11}$$

with the so called heat index I

$$I = \sum_{i=1}^{N} (T_i/5)^{1.514} \tag{12}$$

It is the sum of 12 monthly index values T_i, where T_i is a function of the monthly local normal temperature. Originally, I was assumed to be a constant for each location or grid cell over one year of simulation. This is not applicable for continuous operational estimates with uncompleted years (see improvements below). For monthly estimates of potential evaporation, calculated with equation 10, 30 day months and 12 hour days were assumed and potE_i need to be adjusted for the actual day length. In SLS additional latitude dependent correction factors have been applied to reduce evaporation rates in high latitudes. Mintz and Walker (1993) discussed the fact that the Thornthwaite equation has been developed for temperatures measured under potential conditions and only represents "true" potential evaporation when there is no soil moisture stress. But the land surface temperatures are altered under non-potential conditions. The Thornthwaite method will therefore overestimate the "true" potential evaporation in arid regions.

Taking throughfall, evaporation, soil moisture and snow accumulation into account the SLS generates the appropriate runoff and drainage fields which can be passed down to the discharge module like the comparable output fields of ECHAM climate simulations.

2.1.2 LSXM improvements

The land surface model SLS suffers mainly from the omission of glaciated regions and from the program realization as yearly re-analyses model. The latter is a consequence of the annual formulation of the heat index (equation 12). Further on, important water mass relevant storage fields such as snow infiltration are not saved at the end of one annual simulation cycle. Repeated parameter initializations at each model restart cause discontinuous variations of the total terrestrial water storage.

The recoded land surface model LSXM innovates the original SLS with several essential new features to keep up the vertical water balance even during program stops and restarts. All routines, initializing water storage fields such as soil moisture and infiltration, have been revised. Artificial storage variations due to annual

DOI: 11.2312/GFZ.b103-08095

resets of water holding parameter fields have been eliminated. This requires also a reformulation of the lake and swamp handling. Now, charge-back among dry ground and lakes within one grid cell is enabled. All water mass relevant memory fields of snow and soil water capacities are stored after every time step, prepared for reload and to restart the model on single days.

The estimation of potential evaporation has been enhanced to use a moving 1-year heat index. Independently of the prospective temperature distribution of the rest of the year, it is possible to run the simulation until the actual day of the year. Nevertheless, evaporation remains a critical error source in the global mass balance, because it is the only mass flux in the hydrological cycle that is computed within two different models, atmosphere and hydrology. Both models contain their own land surface component but their results are not synchronized. Unfortunately, the land surface module LSXM included in the hydrological model is necessary as long as the atmospheric models, for instance ECMWF, do not provide the relevant parameter fields, such as soil moisture and snow accumulation, in the same operational manner as precipitation and temperature. As interim solution, LSXM has been enabled to import directly evaporation rates from an atmospheric model. This ensures a consistent mass conservative water exchange among atmosphere and continental surface. The simulation of evaporation rates with the land surface scheme TESSEL (Beljaars & Viterbo, 1999) in the ECMWF weather forecast system benefits notable from the more sophisticated treatment of wind, radiation, and humidity influences compared to the simple temperature based Thornthwaite method in the LSXM. The imported evaporation estimates are higher correlated to local precipitation events. However, water storage distributions still differ between atmospheric and hydrological model estimates. It is not obligatory that the ECMWF evaporation rates fit to surface soil saturation characteristics and local water holding capacities of LSXM. Anyhow, the total vertical water balance keeps comparable and concerning the global water cycle, the terrestrial hydrology is connected more consistently to the atmosphere.

Further efforts were made to incorporate glaciated regions. A simple, seasonal driven annual discharge model has been included to accumulate and remove the annual snow fall. Long-term ice masses are kept constant. This simple model guarantees that no precipitation over glaciers is omitted, and the main part of the seasonal cycle over ice-sheets is captured. The integration of a complex thermo-mechanical ice-sheet model is still an open task in continental hydrology. As demonstrated later, the LSXM succeeds in producing a total vertical water balance that is stable over long periods. All incoming precipitation over land is passed down to the hydrological discharge module as runoff or drainage or back to the atmosphere as evaporation.

2.2 Discharge module HDXM

The Hydrological Discharge eXtended Model HDXM simulates the lateral water fluxes. On the global scale there exist several lateral waterflow processes. Following the HDM model formulation, it is sufficient to classify three different parallel types of flows: overland flow, base flow, and river flow. Water produced within a catchment or grid cell, reaching the land surface by rain or snowmelt as throughfall,

DOI: 11.2312/GFZ.b103-08095

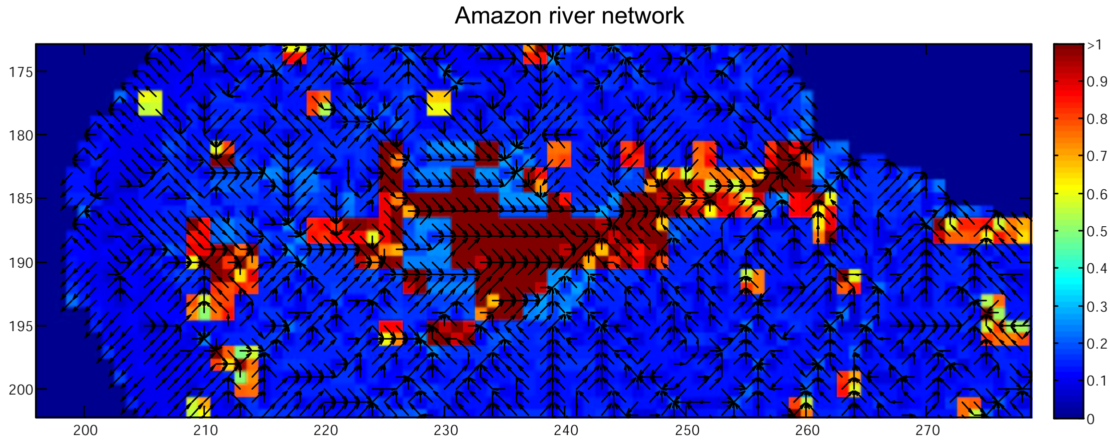

Figure 4. River network for the Amazon. Black arrows: river routing directions; coloured: retention time coefficients for riverflow.

enters the discharge module as surface runoff or groundwater drainage. Surface runoff and interflows can be merged and fed to the overland flow process. Groundwater percolated in the deep soil layers is treated as drainage input for the HDXM. It is passed laterally as base flow. Water entering the catchment from other catchments through the boundaries is transferred by the river network and contributes to the river flow.

2.2.1 Basic HDM

The most obvious water transport system are the rivers. The river network is presented in HDM by a flow direction map, derived from a 5' x 5' topography dataset of the National Geographic Data Centre. One of eight possible outflow directions is allocated to each grid cell of the HDM model. These are the four main directions North, East, South, and West, and the four diagonal directions North-East, South-East, South-West, and North-West (Fig. 4). To validate the HDM flow direction map, comparable simulations, using normalized linear flow reservoirs, were done with the direction schemes of the discharge model TRIP (Total River Integrated Pathways) (Oki et al., 1999) and STN-30 (Simulated Topological Network 30p (Vörösmarty et al., 2000). Calculating HAM time series (see chapter 5), the influence of the flow direction maps has been proved to be below 17% in χ_1 and χ_3, and below 5% in χ_2.

To model retention and translation of water in a flow process, generally a two-parameter approach is required (Hagemann & Dümenil, 1998a). The two parameters represent a cascade of n equal linear reservoirs with retention times k.

The linear reservoir approach can be described by

$$Q_{out} = \frac{S}{k} \tag{13}$$

where the outflow Q_{out} is proportional to its content S. The factor k is called retention coefficient and represents the average residence time or lag time of water within the reservoir (Singh, 1988). According to the global distribution of retention

DOI: 11.2312/GFZ.b103-08095

coefficients, runoff is delayed and water is stored in the flow reservoirs. Sensitivity analyses of Hagemann and Dümenil (2003) turned out that for the representation of overland flow and base flow a single linear reservoir ($n = 1$) is sufficient. River flow needs a cascade of five equal linear reservoirs ($n = 5$). Replacing k from equation 13 the total lag time τ in one grid cell, consisting of a cascade of n linear reservoirs, is simply derived from

$$\tau = n \cdot k \tag{14}$$

For all lateral flow processes the topography is the most important characteristic. For base flow and overland flow the retention coefficients are mainly a function of the average slope and the grid cell length Δx. The mean flow velocity ν is characterized by

$$\nu = \frac{\Delta x}{\tau} \tag{15}$$

The retention coefficients for river flow depend on the topographic gradient and the distance in flow direction. River flow requires calculation with a time step of six hours to pay regard to the minimum travel time through a 0.5° grid cell which is limited by the time step chosen. Wetlands and lakes can be represented with the same flow types, but the retention time parametrization has to be extended by a renewal rate concept. The renewal rate is defined as the ratio of throughput to the average volume within the system (Mitsch & Gosselink, 1993). Because there exist only a few measurements of renewal rates in wetlands and lakes Hagemann and Dümenil developed a conceptual model, representing the influence of wetlands and lakes on the lateral flow process. An additional discharge delay factor f

$$f_{w,l} = 1 - \frac{1}{2}(1 - \frac{\nu_{w,l}}{\nu_0}) \cdot (\tanh(4\pi \cdot (p_{w,l} - p_c)) + 1) \tag{16}$$

accounts for the percental influence of wetlands p_w and lakes p_l. $\nu_{w,l}$ are the flow velocities of overland flow or river flow for a 100% coverage with wetlands or lakes respectively. ν_0 relates to 0% wetlands or lakes according to equation 15. p_c is a threshold value of $p_{w,l}$ corresponding to the decline of $f_{w,l}$ with increasing $p_{w,l}$. Inserting the discharge delay factor in equation 15 one obtains the adjusted retention coefficients from

$$\tau_{w,l} = \frac{\Delta x}{f_{w,l} \cdot \nu_0} \tag{17}$$

As figure 5 shows, the theoretical flow velocities are reduced to the actual velocities in wetland and lake areas. According to their percental coverage the retention times for wetland and lake regions are increased. Wetlands and lakes intercept sharp water flow peaks discharging the water slowly over longer time periods.

2.2.2 HDM extensions

Within the mentioned DFG project TH864/3 the initial version of HDM has been extended to calculate global mass integrals. The vertical water mass balance from

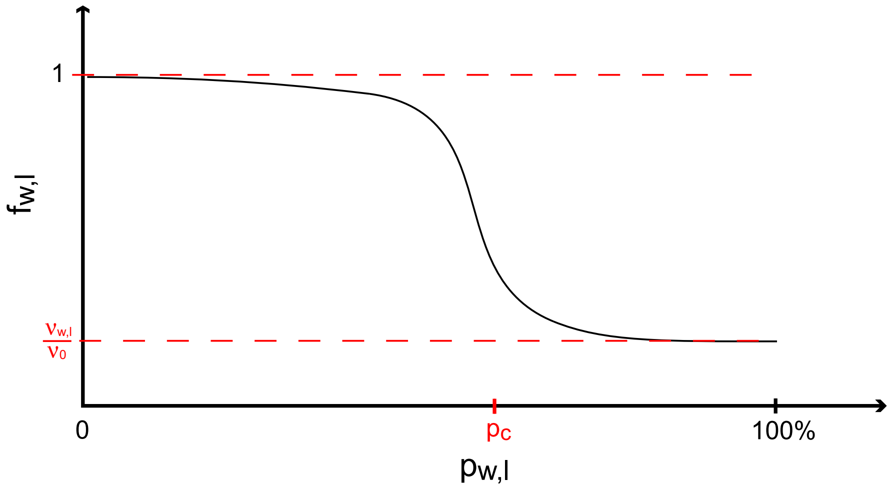

Figure 5. Schematic curve of the discharge delay factor $f_{w,l}$ as function of the grid cell coverage $p_{w,l}$ by wetlands or lakes (Hagemann & Dümenil, 1998b).

the land surface module ($P-E-R-D$) has been included as well as the total water mass storage in each reservoir type. Flow velocities have been estimated from the water budgets and corresponding distances between the grid cells. Following the angular momentum approach for Earth rotation (see chapter 5) variations of the matter and motion term of the hydrological angular momentum (HAM) functions are calculated with a daily time step by integrating the gridded water masses and movements globally over all land surfaces. Additionally, a 3-D topography model has been implemented in order to estimate the sensitivity of the model results with respect to the difference between the topographic heights and a mean Earth radius. The impact of an ellipsoidal geometry has also been tested. Compared to the Earth's radius the topographic height variations are very small. For the calculation of surface mass integrals such as changes of the hydrological tensor of inertia or HAM functions they are usually neglected. The influence of the topography on HAM calculations is generally below 0.03%, while an ellipsoidal geometry causes anomalies up to 0.4% in χ_1, 0.2% in χ_2, and only 0.06% in LOD (Fig. 6). Since these effects are distinctly smaller than other model uncertainties, the spherical approximation of the Earth's shape has been retained unchanged in HDM. In the new HDXM module, described in the next section, an ellipsoidal correction for the calculation of global geodetic parameters has been introduced.

To derive spherical gravity field coefficients from the terrestrial water distribution a subroutine for the expansion of the gravity field into spherical harmonics has been implemented. Because continental water mass variations are restricted to the land surface the expansion into spherical harmonics has to be handled with care (see explanation in chapter 6). In the new HDXM version only the low degree gravity field variations will be computed directly from their mass integrals instead of using the full representation in spherical harmonics.

In combination with the SLS, the HDM exposes several deficiencies concerning mass conservation. The quality of discharge simulations depends not only on the formulations of the model physics and its parametrizations, but also on the precise definition of the land-sea mask (boundaries among land surface, lakes, and oceans).

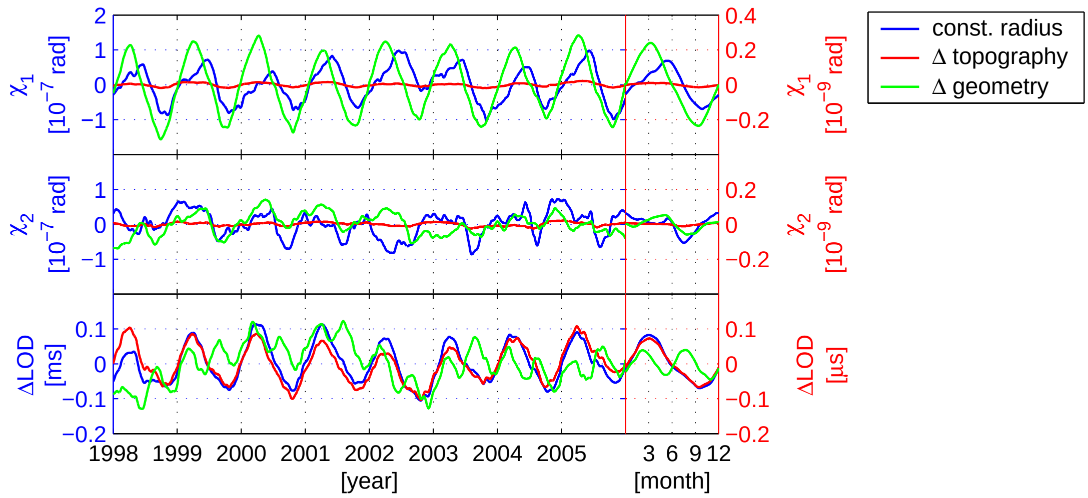

Figure 6. Influence of topography and surface geometry on hydrological angular momentum (HAM) functions (Walter, 2008). HAM time series assuming a constant Earth's radius $R = 6371000m$ (blue). Impact of topographic heights (red). Anomalies resulting from an ellipsoidal approximation of the Earth's shape assuming $R_a = 6378137m$, $R_b = 6356752m$ (green). Blue curve refers to the left y-axis, red and green curve refer to the right y-axis

This is especially true for the estimation of global mass integrals associated with Earth rotation or gravity field variations. Unfortunately, the underlying land-sea masks of SLS and HDM differ and both are neither adjusted to the ocean model nor to the atmospheric model (Fig. 7). HAM results from HDM suffer appreciably from the improper formulation of the land-lake-sea distribution compared to SLS. As a workaround all hydrological simulations had been done only on compatible grid cells so far, although this contradicts the global view of the total continental water mass storage. Omitted water masses had been redistributed to the ocean as a homogeneous layer to ensure internal mass conservation constraints. This approach suppresses notably the retention capacity of snow accumulated in coastal regions in high northern latitudes and also strong precipitation events in the Mid-Asia islands regions.

2.2.3 HDXM improvements

Within the HDXM essential improvements have been made to eliminate the inconsistencies between the former versions of SLS and HDM. Both modules or sub-models, LSXM and HDXM, simulate on the same 0.5° x 0.5° grid, thus runoff and drainage fields can be exchanged without any interpolation. The new recoded HDXM version includes an updated land mask description consistent with the land-lake fraction and the glacier-fraction representation of the LSXM. Parameter fields such as retention times and river routing have been extended accordingly. That update implies also the incorporation of glaciated regions. Aside from Greenland and Antarctica, especially the former unmodelled coastal region of islands in the low latitudes of Mid-Asia are included correctly. The amount of unconsidered land surface areas has been reduced from 11.3% in SLS+HDM (10.8% glaciated regions in high latitudes) to zero. However, the precipitation into a rest of 0.9%

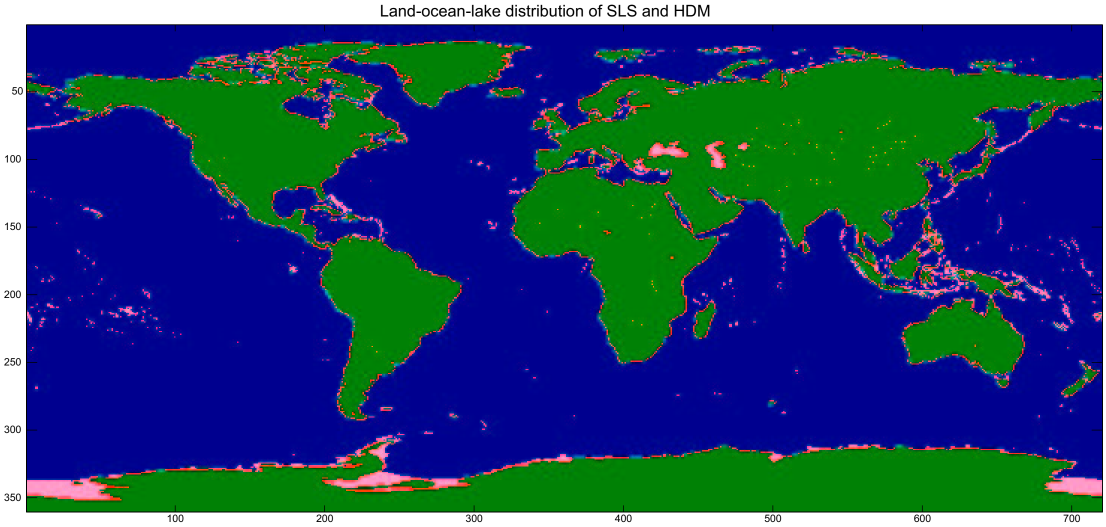

Figure 7. Differences in the land-ocean-lake representation of SLS and HDM sub-models. HDM land consistent with SLS (green). Additional land fractions in SLS (pink). Local dips in HDM (yellow). HDM coast/ocean cells (light blue). HDM coast points defined partly on SLS land fraction (red).

of the land surface, representing a few local dips (65 yellow dots in fig. 7) as well as the "Black Sea" and "Caspian Sea" is still not routed through reservoirs in HDXM. For mass balance purposes the excess of these regions is directly passed through to the ocean as residual water. Compared to the dominant seasonal signal of the directly routed freshwater runoff into the ocean, the unrouted residual water masses are below 12% of the total outcome. Fortunatelly, they contain mainly very high frequency variations contributing marginal to the seasonal signal.

In order to insert hydrology between atmosphere and oceans in a fully mass-conservative way, special attention had to be paid on the mass fluxes among the three models, such as precipitation or evaporation. Small mass losses due to interpolation between the sub-systems are accumulated to artificial long term trends in the tensor of inertia components. The external adaptation of the flux devices is therefore essentially required just as the internal adjustment between the LSXM module and the HDXM module. Additionally to the LSXM and HDXM processing modules a mass conservative remapping tool has been implemented in the LSDM system.

2.3 Mass conservative remapping

Generally, each model (atmosphere, hydrology, ocean) or sub-model (LSM, HDM) has its own optimized spatial and temporal resolutions. Heat, momentum, and mass fluxes among these models need interpolation. Because standard interpolation schemes are not mass conservative, mass losses occur with every interpolation step and the global mass balance is disturbed. First attempts to avoid mass losses related to interpolation were made with the fully coupled climate model ECOCTH (ECHAM5+OMCT+HDM). In ECOCTH a land surface model was already integrated with the comprised climate model ECHAM5. Interpolation became necessary between ECHAM5 and HDM (precipitation, evaporation, runoff, drainage),

DOI: 11.2312/GFZ.b103-08095

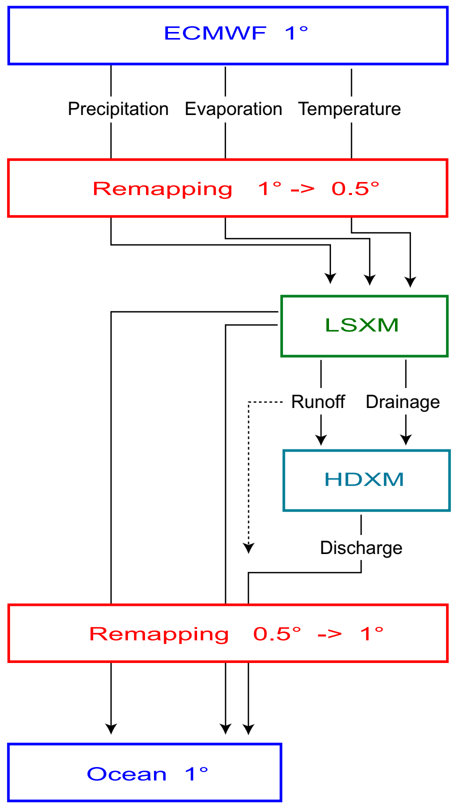

Figure 8. Mass conservative remapping: Balanced mass fluxes for atmosphere, hydrology and ocean model in series.

between ECHAM5 and OMCT (precipitation, evaporation) and between HDM and OMCT (runoff). A supplementary routine has been implemented in ECOCTH which caught the residual water mass losses in the global hydrological cycle. Their sum has been added to the ocean as homogeneous layer. The same approach has been adopted to changes in water masses not considered in the HDM routing scheme, like big continental lakes and local dips. (Sündermann et. al, 2008).

Even with the modelling system LSDM interpolation is not totally avoidable. Interpolation is still necessary between atmosphere and the land surface module LSXM for precipitation and evaporation as well as for the HDXM runoff to the ocean model. General available conservative interpolation routines, covering any interpolation request, are very time-consuming. Therefore, the operational hydrological processing scheme LSDM is at the moment specialised to use only the atmospheric input from the ECMWF model. Adopted to the transformation from the ECMWF grid formulation to the LSDM gridding a suitable fast remapping algorithm has been developed. The restriction to ECMWF input data sets is supported by the fact that also the preferred operational ocean model OMCT applies ECMWF forcing fields. The exact mass-conservative remapping routine transforms ECMWF atmospheric data from a 1° x 1° global grid to the shifted 0.5° x 0.5° sub-grid of LSDM and afterwards back. OMCT, operating on 1.875° x 1.875°, will be updated in the near future to work with the same 1° gridded ECMWF input. Figure 8 illustrates also the possibility to send all mass fluxes from atmosphere through the hydrological model component. This approach guarantees that

DOI: 11.2312/GFZ.b103-08095

no masses are lost due to unadjusted land-sea masks of LSDM and ocean model. Following this concept the water masses can be exchanged consistently among the involved atmospheric, oceanic, and hydrological models.

2.4 Implementation of an operational hydrological processing scheme

The code of the hydrological model LSDM has been optimized for fast and stable daily simulation steps. The exact status of all water mass related parameter fields in LSXM and HDXM is preserved from one simulation run to subsequent runs. Preprocessing steps have been implemented to prepare the operational 6h atmospheric fields from ECMWF for the required daily accumulative precipitation and evaporation input and for the daily mean temperature fields. The total freshwater outcome after the LSDM simulation, including water masses not routed in the HDXM module, is prepared in a post-processing step to obtain the continental discharge flux in an appropriate format for further application in OMCT. The whole processing scheme (Fig. 9), starting from the collection of input fields from ECMWF until output of global geodetic parameters and their retrieval per public FTP, is embedded in automated scripts at the German High Performance Computing Centre for Climate and Earth System Research (DKRZ) in Hamburg. The scripts are managed and monitored from GFZ. Rigorous error detection routines guarantee automatic stopping and restart of the operational processing in case of disability of the involved computer service centres at ECMWF, DKRZ and GFZ.

For the future it is planed to provide the complete output, HAM, water mass

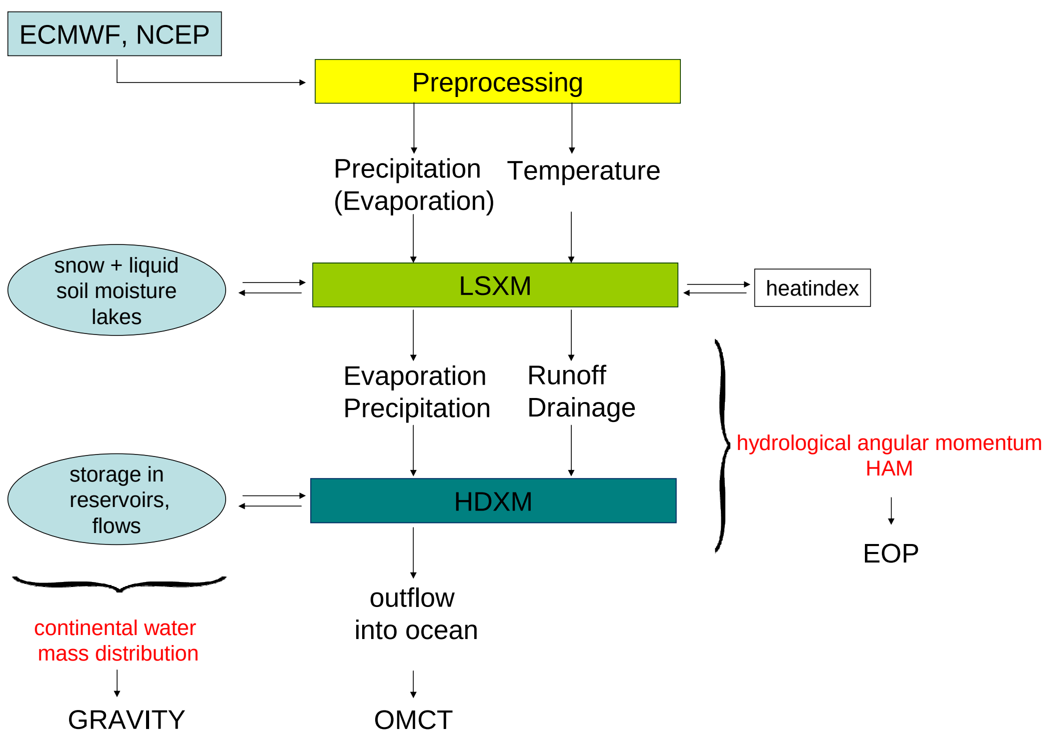

Figure 9. Flow chart of the operational LSDM processing scheme.

storage, and continental discharge, allocated at an appropriate data centre portal. As a quick fix a fraction of the daily updated LSDM output files is available via public anonymous FTP at GFZ.

`FTP.GFZ-POTSDAM.DE public/ig/dill`

The output files for the hydrological angular momentum (HAM) time series contain the following variables:

- hydrological angular momentum motion term of χ_1,χ_2,χ_3
- hydrological angular momentum matter term of χ_1,χ_2,χ_3
- low degree gravity variations: C_{10}, C_{11}, C_{12}, C_{20}, C_{21}, S_{21}, C_{22}, S_{22}

Beside the file of the actual year, consistently reprocessed output files for the ERA-40 period (1958-2000) and the operational ECMWF analyses since 2001 are also available. Additionally, an approximated estimation of the indirect hydrological effect can be downloaded, too (see further explanations below). More information on format and content of the provided time series is attached in a README-file.

2.5 Indirect hydrological effect

The operational hydrological simulation results, presented above, are tailored to the combination with ECMWF atmospheric simulations and ECMWF forced oceanic simulations. To close the global water balance, it is also mandatory to consider the indirect hydrological effect caused by freshwater fluxes from the continental hydrology into the ocean. Neglecting the continental freshwater runoff into the oceans can lead to amplified effects in the global geodetic parameters which are cancelled out otherwise. Especially the length of day variation (ΔLOD) is very sensitive for this indirect hydrological effect. The continental runoff produces an increased annual amplitude and, in addition, a phase shift of the annual signal of about 70° in ΔLOD (Walter, 2008). Preliminary examinations of the impact of river discharge on global ocean mass distributions have been arranged with ECMWF forced OMCT simulations including runoff from the HDM model (Dobslaw & Thomas, 2007). While the sub-monthly mass variability was generally insignificant for GRACE de-aliasing purposes in most oceanic regions, monthly mean mass signals of up to 2hPa occur in the Arctic Ocean during the melt season. Additionally, from total freshwater fluxes due to precipitation, evaporation, and river discharge seasonal variations of the total ocean mass have been calculated. Their good agreement with estimates based on GRACE observations suggest that the consistent treatment of the indirect hydrological effect is essential for the generation of realistic mass redistributions among the three Earth subsystems atmosphere, ocean, and continents.

Typically, public available oceanic angular momentum (OAM) variations are produced without any freshwater exchanges among land surface and oceans. Since most oceanic models treat the ocean mass or volume as constant total Earth rotation excitation estimates from AAM (atmospheric angular momentum), OAM, and HAM combinations as well as corresponding gravity field variations suffer from the disregard of the indirect hydrological effect.

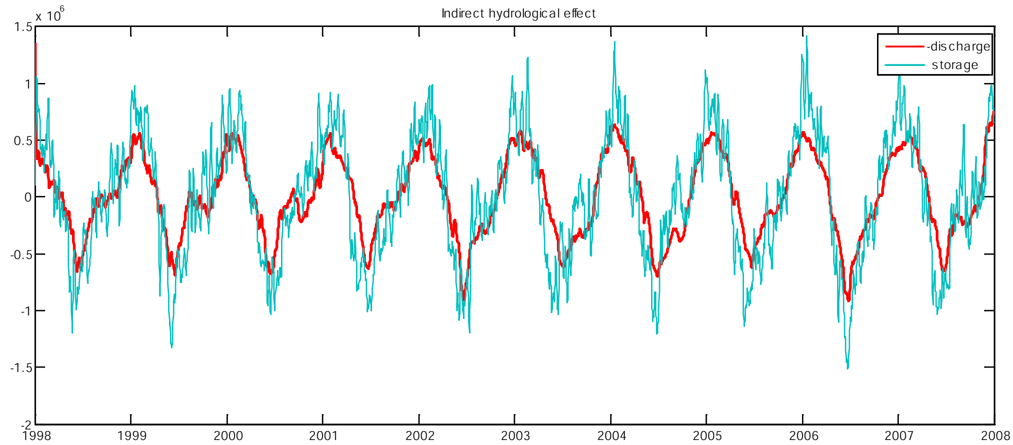

Figure 10. Indirect hydrological effect: Total continental discharge into ocean (red) and continental storage variation (light-blue) in $[m^3/s]$, simulated with LSDM. Both time series are detrended for comparison.

To get a closed picture of the global geodetic parameters the missing influence of the continental runoff on oceanic mass distributions has to be calculated separately. Assuming that freshwater fluxes into the ocean have no effect on the oceans general circulation the continental freshwater runoff is distributed instantaneously over the ocean, approximated with an additional homogeneous layer. In order to avoid long-term trends of the ocean mass, considering only seasonal runoff variations, one has to apply some kind of linear reduction to this additional ocean layer. This can be done for instance by fitting piece-wise linear annual trends and subtract them. Unfortunately, the resulting continuous removal of water out of the ocean did not correspond to the ECMWF atmosphere-ocean budget (difference of precipitation and evaporation over oceans). The remaining positive trend of the total ocean mass is owing to deficiencies in the ECMWF based atmosphere-ocean flux balance.

Another common workaround is to derive the indirect hydrological effect by distributing the total continental water storage variation inversely over the ocean. However, that approach assumes a negligible effect of total mass variations in the atmosphere. The major part of the difference between mass variations of the continental storage and the continental discharge (Fig. 10) represents atmospheric mass variations due to the atmosphere-land budget (difference of precipitation and evaporation over land surfaces).

In fact the atmospheric mass variations are very small compared to the terrestrial hydrological ones (Van Hylckama, 1970). Keeping the atmospheric mass constant this approach cancels out the atmosphere-ocean budget with the atmosphere-land budget. Analyses of the total atmospheric budget from ECMWF simulations exposes not only small atmospheric mass variations but also an unbalanced total atmospheric water mass reflected in a long-term trend. In the ECMWF assimilation scheme it is not mandatory that the prognostic atmospheric mass variation matches the diagnostic mass exchange due to precipitation and evaporation. Further efforts are needed to adjust the total atmospheric precipitation fields to a realistic ocean-atmosphere balance.

Figure 11 shows calculations of the total global water storage for ERA-40 re-

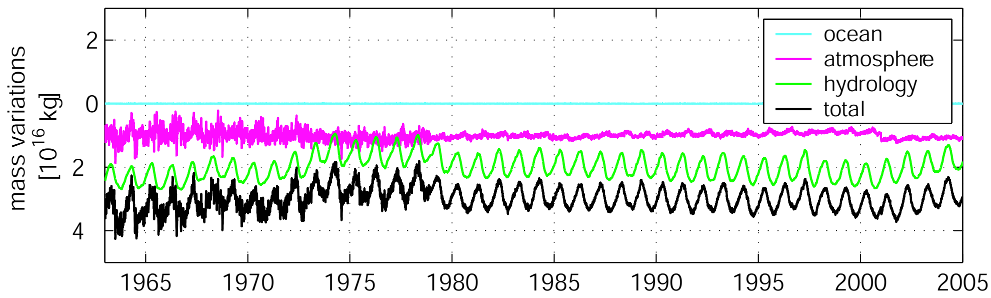

Figure 11. Variation of global water masses of ocean, atmosphere, hydrology and sum of all, simulated with ECMWF and SLS+HDM. For better readability the curves are arbitrary shifted by $-10^{16}kg$.

analyses data and corresponding LSDM simulations. The applied ocean model OMCT treats the ocean mass as constant. The most obvious mass variations come from hydrology with annual amplitudes of $3.83 \cdot 10^{15}kg$. Due to its storage capability the continental hydrology produces significant runoff delays reflected particularly on seasonal time scales. The atmosphere shows much lower seasonal variations with amplitudes of $0.46 \cdot 10^{15}kg$. It can also be seen that the variability of high-frequency noise in the continental hydrosphere is reduced with the introduction of satellite measurements in the ECMWF assimilation technique since 1979. The change from ERA-40 to operational data of ECMWF in 2001 is accompanied by a discontinuity in total atmospheric mass and a slight trend in hydrology. The changing implementation of VTPR (Vertical Temperature Profile Radiometer) data in the period 1973 - 1978 also affects the global water contents adversely.

The combination of direct HAM functions and HAMs induced by the indirect effect through freshwater fluxes into the ocean shows that these two processes partly compensate due to opposite amplitudes in polar motion. An amplified effect appears in ΔLOD due to its direct dependency on the total water mass in the system.

3 VALIDATION OF SIMULATED CONTINENTAL DISCHARGE

Simulations of continental discharge with LSDM strongly depend on the applied atmospheric forcing, primarily the precipitation data. This dependency is even more pronounced when evaporation rates from the LSXM module are used instead of those provided by ECHAM or ECMWF. The latter comprehend of a much more complex land surface modelling including humidity, radiation and wind parameters. The consistent use of precipitation and evaporation from one single land surface model, as realized now in LSDM, also considerably reduces precipitation overestimations. Monthly precipitation means from the atmospheric models (ECHAM, ECMWF, NCEP) were compared with observed climatological values from the Global Precipitation Climate Centre (GPCC). NCEP re-analyses overestimate notably precipitation rates in the first half of the year over the northern hemisphere. ECHAM and ECMWF slightly underestimate precipitation in tropical regions such as the Amazon and Orinoco basin (Fig. 12). For all simulation models the monsoon precipitation in India is too low. In contrast, the models generally

DOI: 11.2312/GFZ.b103-08095

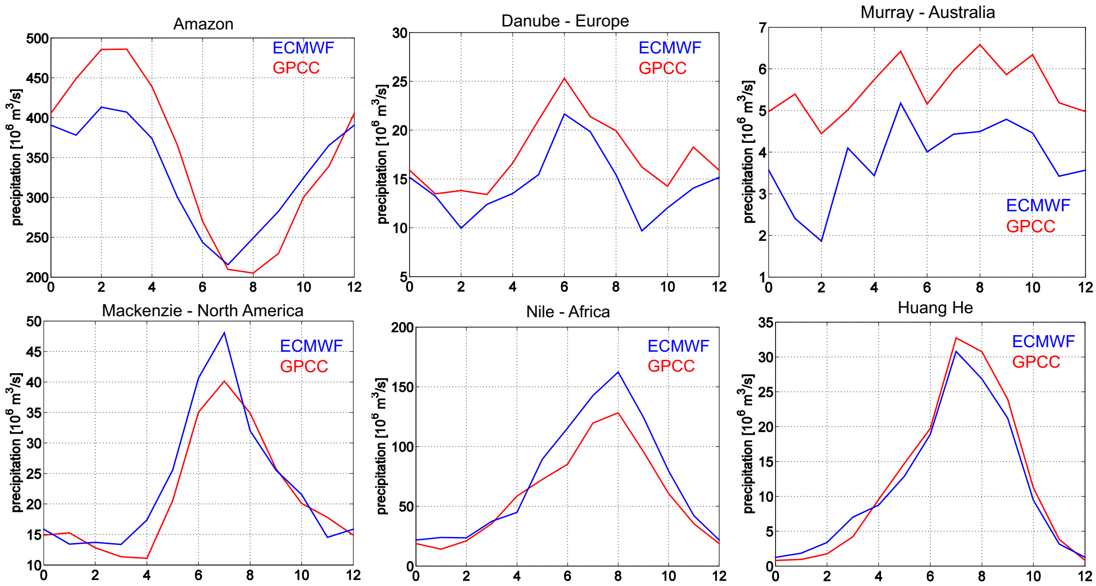

Figure 12. Monthly precipitation means in the river basins of Amazon, Danube, Murray, Mackenzie, Nile, and Huang He as derived from GPCC observations (red) and ECMWF estimates (blue).

overestimate precipitation in spring over the northern hemisphere. The ERA-40 precipitation rates include a positive trend until 1978 correlated with parameter changes in the assimilation background model. In total, the correlation of monthly mean precipitation rates from GPCC with NCEP re-analyses is 0.9, with ERA-40 0.8, and with the unconstrained climate model ECHAM4 0.4. A detailed description including a principal component analysis of the different atmospheric forcing fields can be found in the PHD-thesis of Walter (2008).

Due to the lack of globally distributed water storage measurements the LSDM

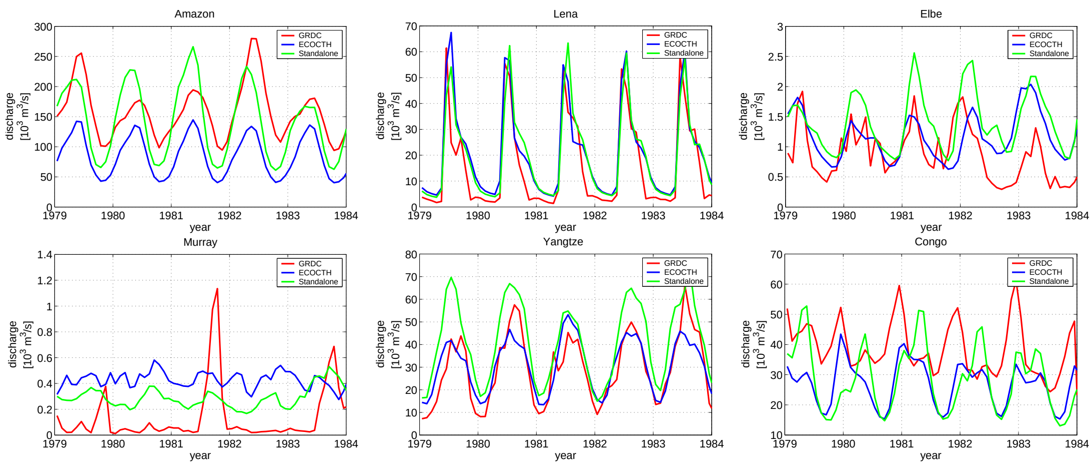

Figure 13. River discharges of Amazon, Lena, Elbe, Murray, Yangtze, and Congo as derived from GRDC observations (red), HDM simulations forced with ECHAM5 precipitation rates (green), and discharges estimated with the dynamically coupled system model ECOCTH, including also HDM (blue).

can only be validated indirectly via modelled river discharges and in-situ river discharge measurements. A detailed verification of river discharges as simulated with LSDM, forced with ERA-40 (1958-2001) and operational ECMWF analyses (2000-2007) has been done by Griesbach (2004) and Walter (2008). Based on statistical analyses they compared simulated river discharge results with documented runoff data at 142 selected stations from the Global Runoff Data Centre (GRDC). Within the mentioned DFG research project TH864/3 similar comparisons have also been done with HDM stand-alone runs forced with ECHAM5 and with ECOCTH simulations. Since the changes from SLS+HDM to LSDM do not effect the general river discharge characteristics the results of these studies can be transferred to the new operational model version. Most noticeable are the undervalued river discharges in low latitudes, caused by too low precipitation rates, like in the Amazon or Congo basin (Fig. 13). On the other hand, all Arctic river catchments are in good agreement with the GRDC measurements. Rivers determined by high evaporation rates and extensive human water consumption, like Murray in Australia, are represented insufficiently. Due to the absence of anthropogenic influences in the HDM and LSDM model only nature-oriented river catchments produce meaningful discharge simulations.

4 VALIDATION OF THE CONTINENTAL HYDROLOGICAL BUDGET

Long-term simulations of global geodetic parameters are very sensitive to small deficiencies in the global mass balance. In principal, the hydrological model should pass down the surplus from precipitation and evaporation over land surfaces from the atmosphere to the ocean. Over longer periods the continental mass variations should accumulate around zero. The global sum of total continental water storage variability has been checked to prove the desired balanced behaviour for the LSDM model. Figure 14 gives the global sums of continental water storage and the related water mass fluxes precipitation, evaporation, and discharge into the oceans

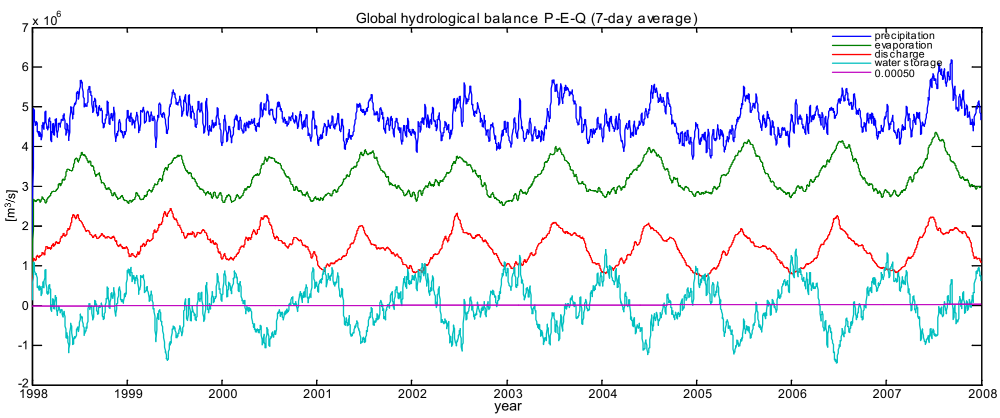

Figure 14. Global sums of precipitation (blue), evaporation (green), discharge (red) and their sum as continental water storage variation (light blue) (7-day averages). The trend of the continental water storage (pink) is negligible with 0.0005 m^3/s over 10 years.

DOI: 11.2312/GFZ.b103-08095

for 1998-2008. Both, precipitation and evaporation, reflect dominant seasonal signals. Their seasonal correlation refers to the combined estimation of both fluxes within one land surface model. The excess budget, from precipitation and evaporation, routed over the land surface leads to the discharge time series. It reflects seasonal maxima in late spring due to snow melt and delayed runoff characteristics in summer due to retention processes of continental reservoirs. The terrestrial water storage is calculated from the global continental budget $(P - E - Q)$. As expected it expresses snow accumulations during the winter period in the northern hemisphere, followed by a minimum after the melt season in early summer.

Considering the trend, the total water storage is balanced. Regional analyses detect negligible negative trends for the Antarctic and the Arctic regions whereas the global trend is marginal positive. Whether these signals are real or artificial has to be analysed in more detail, particularly with long term climatological atmospheric forcing. Since a sophisticated ice model is still missing in LSDM, reliable climatological conclusions are not possible. Concerning the medium-term behaviour of LSDM the continental hydrological budget performs reasonable. The negligible global trend of 0.00005 m^3/s per year has no influence on the estimation of the following global geodetic parameters.

5 HYDROLOGICAL ANGULAR MOMENTUM, HAM

Following the widely used angular momentum approach (Wahr, 1983; Schmitz-Hübsch & Dill, 2001), hydrological induced Earth rotation parameters (ERP) for polar motion and length of day variations can be derived from hydrological angular momentum (HAM) functions. The HAM functions serve as excitation input for a gyroscopic Earth model responding with Earth rotation variations in terms of ERPs. Instead of comparing ERPs, HAM time series of different models can be compared independently of the precise modelling of the Earth eigenfrequencies such as the Chandler wobble. HAM functions can be separated into a matter term related to static mass variations and a motion term related to mass motions relative to the rotating terrestrial reference frame. The matter term of HAM functions expresses changes of the tensor of inertia components, I_{13} and I_{23} for polar motion, and I_{33} for length of day variations. Therefore, it is also related directly to degree 2 gravity coefficients. In LSDM the whole tensor of inertia is calculated daily from surface integrals of the vertical and lateral water balances. Additional correction factors, applied to the HAM matter term, account for the influences of rotational deformation, coupling of the Earth's core and mantle, and surface deformations due to loading effects. The motion term of the HAM functions is obtained from the velocities of water masses in all flow processes relative to the Earth's rotation. Detailed information on the applied angular momentum approach and the involved correction factors can be found in the README-file on the FTP server.

HAM time series of the routinely operational LSDM simulation (model-3) have been compared with results from former stages of development, namely the original SLS+HDM (model-1) and LSDM (model-2) with evaporation estimates from LSXM instead of evaporation rates from ECMWF (Fig. 15).

Most obvious are the differences between model-2 and model-3. Since the evap-

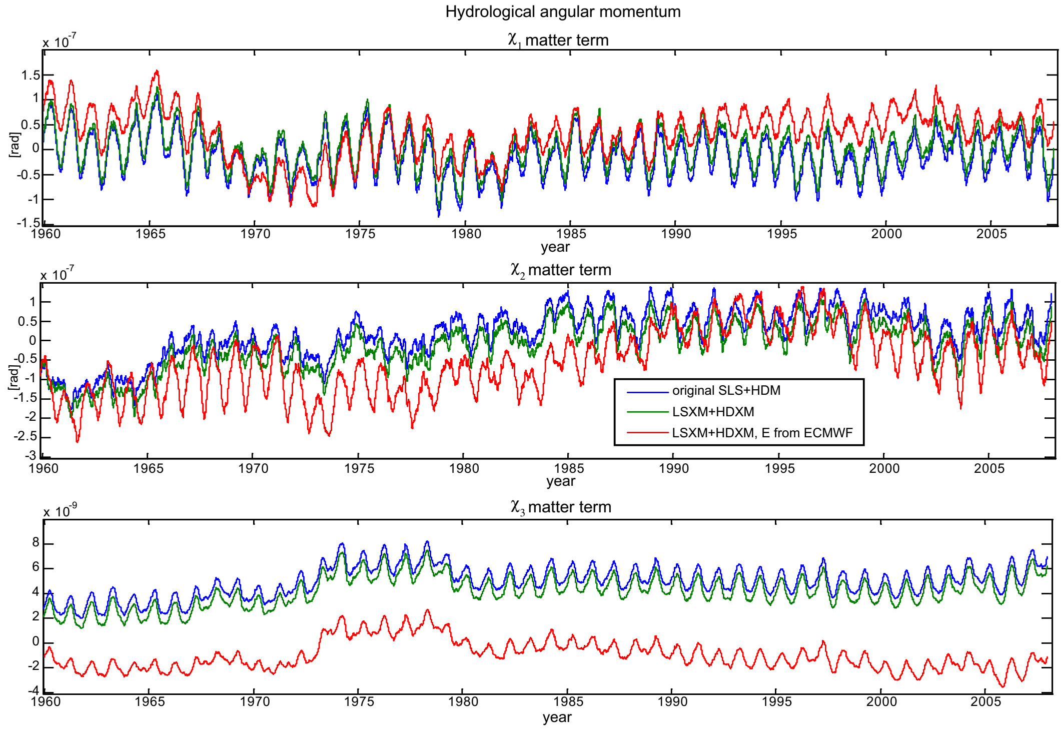

Figure 15. Hydrological angular momentum functions (matter term) as derived from three distinct simulations forced with ECMWF data, 1960-2007. Simulation with original SLS+HDM (blue), with LSDM using internally calculated evaporation rates (green), and LSDM with evaporation rates imported from ECMWF (red).

oration rates imported from ECMWF analyses are much higher than the one calculated internally with the LSXM module, the overall continental water storage level becomes lower for operational simulations with model-3 than with model-2. The overestimated precipitation from operational ECMWF analyses in spring over the northern hemisphere is somewhat compensated by the corresponding higher evaporation rates. This refers to the correlation of increased evaporation with increased humidity due to precipitation. The downgraded continental water storage is considerably reflected in an offset of the χ_3-component. Corresponding to the reduced total annual water variations the χ_3-amplitude is slightly reduced, too.

Another more surprising effect occurs for the ECMWF operational time period. The trend, appearing since 2000 in the former simulations (model-1, model-2), almost vanishes when using evaporation as input from the operational ECMWF analyses. The common use of precipitation and evaporation from one single land surface model yields a more realistic global atmosphere-land budget (difference between precipitation and evaporation) than combining ECMWF precipitation rates with evaporation rates from LSXM. It is supposed that errors in the ECMWF estimation of precipitation are partly cancelled by correlated evaporation rates. In contrast to the global behaviour of the total continental water storage, expressed in the axial component, the different evaporation rates of model-2 and model-3 pronounce somehow individual precipitation events in mid-latitudes. The equatorial components χ_1 and χ_2, more sensitive to regional water storage variations, show higher seasonal variability expressed in increased annual amplitudes. Additionally,

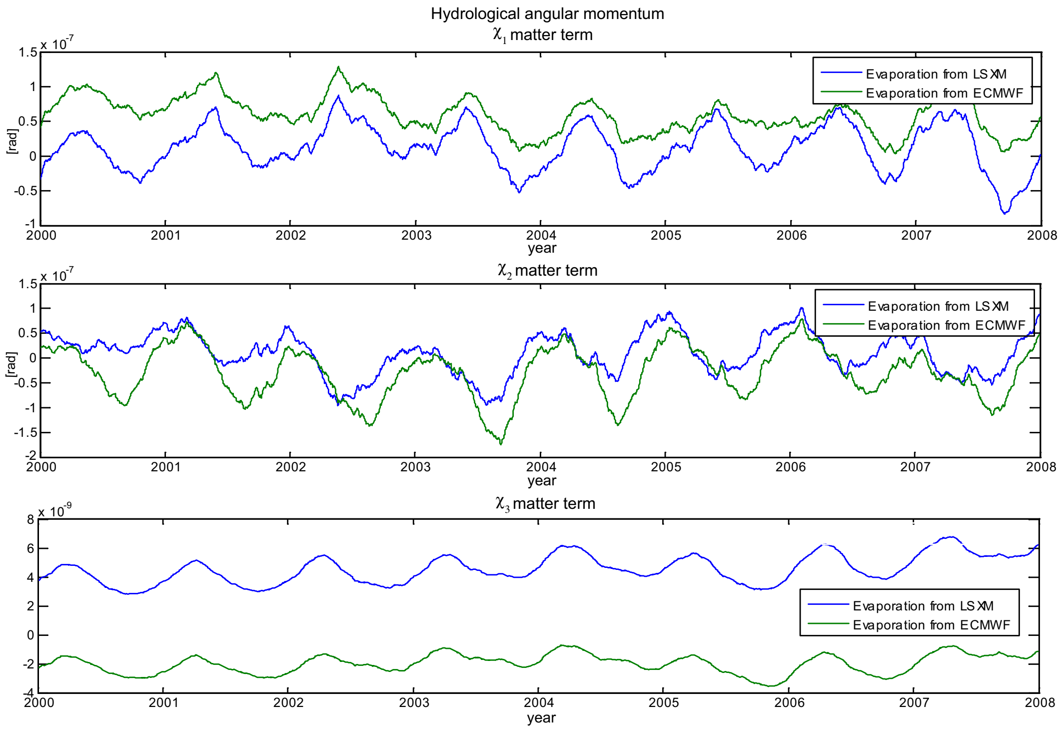

Figure 16. Same as figure 15, zoom in time period 2000-2007 of operational ECMWF analyses.

the phase of the χ_2-component is apparently delayed by 1-2 month (Fig. 16).

Oppositely to the polar motion matter terms, the amplitudes of the motion term are slightly reduced (Fig. 17). The seasonal motion term is mainly caused in regions with high velocities and high topographic gradients of the river flow. They do not necessarily correspond to the regions which are most sensitive for the polar motion matter term. As expected, the river flow maxima occur after spring at the end of the melting season.

Generally, the operational HAM time series from LSDM, model-3, look comparable in amplitude and phase to the former results. The dominant influence of the precipitation input from ECMWF is slightly reduced by the incorporation of

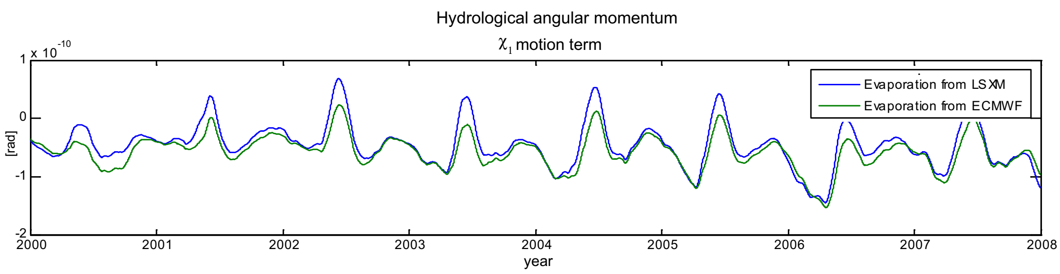

Figure 17. Comparison of HAM motion term as derived from simulations forced with ECMWF data, 2000 - 2007. Results from LSDM using internally calculated evaporation with LSXM (blue), and from LSDM with evaporation rates imported from ECMWF (green).

evaporation estimates from the same atmospheric forcing model, particularly for the period of operational ECMWF analyses since 2001.

Recent comparisons of the total angular momentum excitation budget from AAM, OAM, and HAM with observed ERPs from the International Earth Rotation and Reference System Service (IERS) show also that the new HAMs from the LSDM (model-3) fit better into the required total excitation (pers. communication with A. Groetzsch, 2008). In conclusion, the presented operational HAM time series offer the possibility to use simulated hydrological excitation parameters for reduction and de-aliasing applications of observed ERPs. The public availability of the operational results should stimulate the scientific community for further investigations in Earth rotation analyses.

6 COMPARISON OF SIMULATED AND OBSERVED C_{20} GRAVITY COEFFICIENTS

Observations of the time variable gravity field with the Gravity Recovery Climate Experiment (GRACE) satellite mission provide the possibility to compare monthly GRACE spherical harmonics of terrestrial water storage variations with simulated gravity field variations from hydrological models. Attention should be paid to the restriction of the hydrological water masses to the continental surface. Any expansion of the global gravity field in spherical harmonics cannot resolve the coastal discontinuities. In consequence, the spherical harmonic approach can cause leakage effects into the oceans.

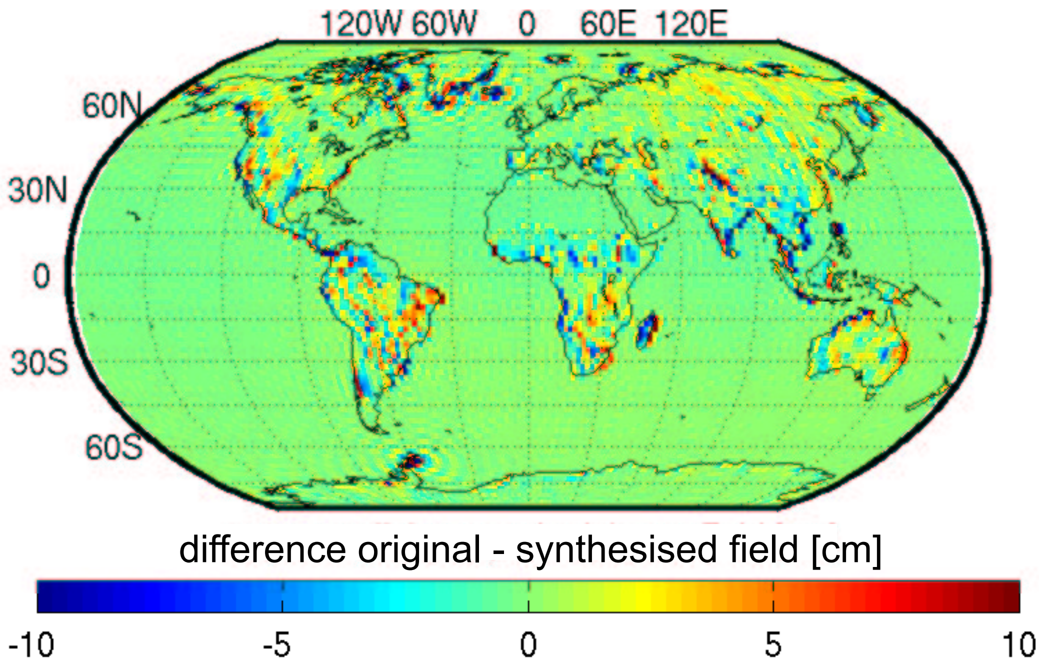

Figure 18. Differences between water mass storage, calculated from HDM and from a synthesised gravity field via spherical harmonic coefficients for April 1990, expressed in equivalent water heights [cm].

DOI: 11.2312/GFZ.b103-08095

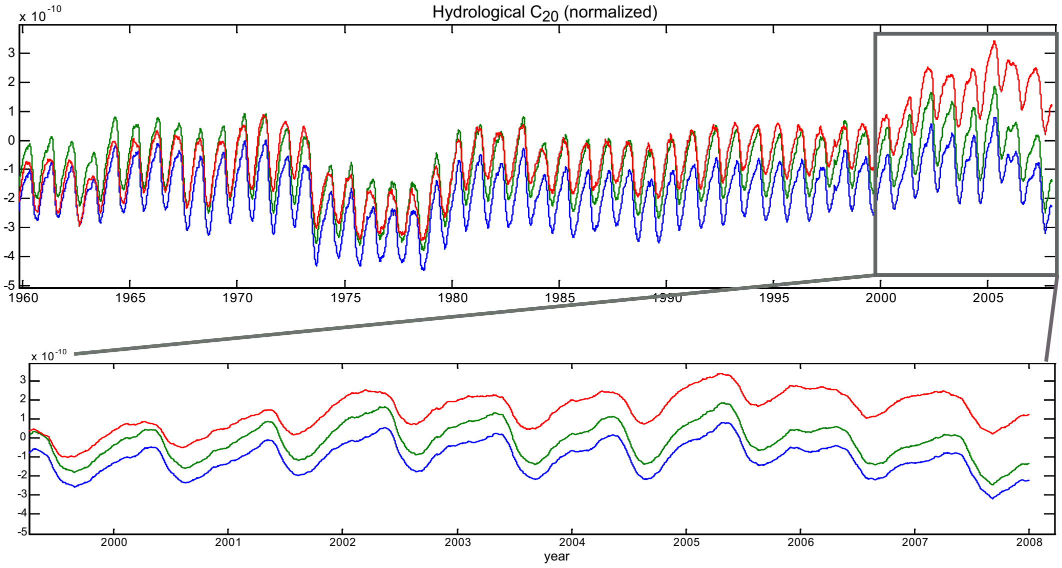

Figure 19. Comparison of C_{20} gravity variations simulated with ECMWF forced hydrological models, 1960-2007: original SLS+HDM (blue), LSDM using internally calculated evaporation with LSXM (green), and LSDM with evaporation rates imported from ECMWF (red).

Large mass variations near coastal river basins may leak into estimates of ocean mass variations and vice versa, resulting in additional artificial mass signals. The differences between actual water mass distribution and synthesized masses retrieved from a spherical harmonic representation might add up to 10 cm equivalent water heights (Fig. 18).

Despite the problems of representing the continental water mass variations as spherical harmonics, individual gravity field coefficients can be calculated directly via their mass integrals. The operational LSDM hydrological model provides daily low degree spherical harmonic coefficients for C_{10}, C_{11}, C_{12}, C_{20}, C_{21}, S_{21}, C_{22} and S_{22}. Since the tensor of inertia elements I_{13} and I_{23} are directly connected to C_{21} and S_{21}, the analysis of the HAM polar motion matter terms χ_1 and χ_2 can be transferred to these gravity coefficients. The following investigations concentrate on the C_{20} coefficient. It is related to the total global water balance and to ΔLOD and therefore qualified as control parameter to check mass budget consistencies. In the majority of cases miss-modelled water fluxes causing regional water budget errors show up as trends in C_{20}. Figure 19 gives the normalized C_{20} coefficient for three different model stages for the period 1960 - 2008. Whereas the operational LSDM (model-3, using the ECMWF evaporation rates) correlates very well with the former LSDM (model-2, using the LSXM evaporation estimates) for the ERA-40 period until 2000, the two simulation results differ significantly for the operational ECMWF period from 2000 until now. Starting with a strong increase until mid of 2002, C_{20} from model-2 decreases since 2005. The increase is even more pronounced for results from model-3, the decrease is weaker. Until 2000 the ERA-40 re-analyses data from ECMWF seem to contain evaporation rates comparable with evaporation estimates from the internal LSXM module. In contrast, the evaporation estimates from the operational ECMWF analyses indicate much more

DOI: 11.2312/GFZ.b103-08095

variability from 2000 on. This may be a consequence of the implementation of new land surface processes and changes in the model parametrization of ECMWF.

C_{20} is dominated by seasonal signals. One conventional analysis approach is to fit the time series with a superposition of an annual and a semi-annual signal. Equation 18 gives the adjusted sine functions with annual and semi-annual amplitude A_1, A_2 and their corresponding phases p_1, p_2.

$$A_1 * sin(2\pi \frac{t}{T_1} + p_1) + A_2 * sin(2\pi \frac{t}{T_2} + p_2) \tag{18}$$

T_1 and T_2 are the annual and semi-annual periods respectively. Rewriting equation 18 in terms of sine and cosine functions, five harmonic parameters have been estimated within a least squares adjustment according to

$$fit(t) = P_1 + P_2 * sin(\omega) + P_3 * cos(\omega) + P_4 * sin(2\omega) + P_5 * cos(2\omega) \tag{19}$$

with $\omega = 2\pi \cdot 1/365.25$. From the fitted parameters P_2 to P_5 in equation 19 the annual and semi-annual amplitudes can be obtained by

$$A_1 = \sqrt{P_2^2 + P_3^2} \qquad A_2 = \sqrt{P_4^2 + P_5^2}$$

and the corresponding annual and semi-annual phases are

$$tan(p_1) = \frac{P_3}{P_2} \qquad tan(p_2) = \frac{P_5}{P_4}$$

For comparison, this harmonic analysis has been done for three different stages of development of the LSDM model (model 1-3). In table 2 the analyses of C_{20} time series from the satellite observations LAGEOS and GRACE and the results from the hydrological model WGHM (WaterGAP Global Hydrology Model) (Alcamo et al., 2003; Döll et al., 2003) are also listed (pers. communication with F. Flechtner, 2008).

C_{20} [$\cdot 10^{10}$]	LAGEOS	GRACE	WGHM	SLS+HDM	LSDM E from LSXM	LSDM E from ECMWF
Ampl. (annual)	1.28	0.65	0.70	0.93	1.02	0.77
phase (annual)	45.2	59.2	39.6	8.5	11.4	25.1
Ampl. (semi-a)	0.61	0.35	0.15	0.44	0.44	0.30
phase (semi-a)	-73.3	-47.1	42.1	-9.9	-4.4	1.3

Table 2. Annual and semi-annual amplitudes and phases in hydrological induced C_{20} variations for 2001-2005, GRACE 2002-2006.

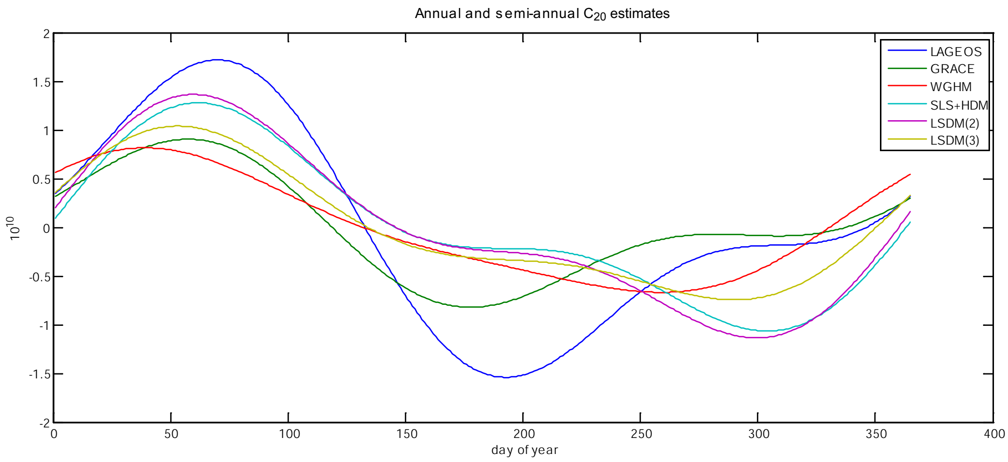

Figure 20. Synthesized annual and semi-annual signal, fitted to C_{20} estimates by harmonic analysis of satellite observations LAGEOS (blue) and GRACE (green) and hydrological models WGHM (red), LSDM model-2 with evaporation rates from LSXM (purple), and LSDM model-3 with evaporation rates from ECMWF (yellow).

The development from the initial SLS+HDM model to the operational LSDM indicates a continuous improvement in the annual amplitude and phase towards the results from GRACE and WGHM. The semi-annual amplitude agrees also very well. The semi-annual phases seem to be not very reasonable among all results. The deficiencies in the semi-annual phase estimates produce a differing synthesized seasonal signal from the beginning of the second half of the year, particularly between satellite observations and hydrological models (Fig. 20). The remaining differences are caused by errors in the hydrological models as well as by errors in the background models applied for GRACE data processing. It might be stressed, that any harmonic analysis suffers from periodic but not ideally sinusoidal signals in the time series. Due to snow accumulation, melting, and retention processes the hydrological mass variations are sometimes better illustrated by saw-tooth functions. Any harmonic decomposition of such a signal will result in artificial power shifted to high harmonics. Restricting the harmonic analysis to only one inter-annual period, the semi-annual one, causes unpredictable approximation errors. In contrast to the annual period, the semi-annual signal is therefore not very distinct. Especially the phase estimates are very sensitive to minor changes in the harmonic decomposition.

7 CONCLUSIONS

The operational hydrological modelling system LSDM consists of an improved land surface module LSXM and the enhanced discharge module HDXM, embedded in mass conserving ECMWF specific pre- and post-processing algorithms. LSDM is capable of reproducing daily continental water mass variations on a global scale in near-real time. The good agreement of modelled gravity field variations with estimates based on GRACE observations suggest that the combined system of ECMWF, OMCT, and LSDM represents consistently water mass redistributions among the three Earth subsystems atmosphere, oceans, and continental hydro-

DOI: 11.2312/GFZ.b103-08095

sphere, in particular on seasonal time scales. The seasonal cycle is captured very well. Furthermore, the total global water budget keeps balanced. The adjustment of the discharge module HDXM to the land-ocean representation of the land surface module LSXM, the incorporation of glaciated regions, and the introduction of mass-conservative remapping leads to significant improvements of modelled global geodetic parameters such as angular momentum variations and low degree gravity field changes. The adoption of evaporation rates from the applied atmospheric model ECMWF avoids mass losses during the land surface processing and additionally compensates errors in the precipitation forcing data. Though the water balance over glaciated regions could be closed with a primitive snow model, a more sophisticated treatment of precipitation over glaciers as well as the consideration of ice mass transports are still needed. As recently as a convenient ice model closes this gap in the hydrological cycle, the coupled hydrospheric model system ECMWF-OMCT-LSDM would be able to supply reliable estimates of persistent water mass redistributions at present time via the combined analyses of observed and simulated global geodetic parameters.

ACKNOWLEDGMENT

This research was based on studies supported by the Deutsche Forschungsgemeinschaft (DFG, German Research Foundation) as part of the projects "Earth System Model" under grant TH864/3 and "Earth rotation and the ocean's circulation" under grant TH864/7-1 within the research unit FOR584 "Earth rotation and global dynamic processes". We are grateful to the Deutsches KlimaRechenZentrum (DKRZ) for supporting computer and network facilities, to the Max-Planck-Institute (MPI) Hamburg for the original code of the SLS and HDM models and to F. Flechtner from GFZ for providing comparable GRACE and WGHM results.

REFERENCES

Alcamo, J., Döll, P. ,Henrichs, T. ,Kaspar, F. ,Lehner, B. ,Rösch, T. , Siebert, S., 2003. Development and testing of the WaterGAP2 global model of water use and availability. *Hydrological Sciences* **48(3)**, pp. 317-337.

Beljaars, A.C.M., Viterbo, P., 1999. Soil moisture-precipitation interaction: Experience with two land surface schemes in the ECMWF model. In: Browning, K., Gurney, R. (ed) *Global energy and water cycles*, Cambridge University Press, Cambridge, pp. 223-233.

Bergström, S., 1992. The HBV model - its structure and applications. *Swedish Meteorological and Hydrological Inst.* Rep. **4**

Bliss, N.B., Olsen, L.M., 1996. Development of a 30-arc-second digital elevation model of South America. *Pecora Thirteen, human interactions with the environment - perspectives from space.* Sioux Falls, South Dakota, USA, pp. 20-22.

Chebotarev, A.I., 1977. 364 - Comp. of meteorology Vol. II: Part 1 - General Hydrology. *World Meteorological Organisation*, Geneva, p. 23.

Dobslaw, H., Thomas, M., 2007. The impact of river run-off on global ocean mass redistribution. *Geophys. J. Int.* **168**, pp. 527-532.

Döll, P., Kaspar, F. ,Lehner, B., 2003. A global hydrological model for deriving water availability indicators: model tuning and validation. *Journal of Hydrology*, **270**, pp. 105 - 134.

Dümenil, L., Todini, E., 1992. A rainfall-runoff scheme for use in the Hamburg climate model. In: Kane, J.P. (ed) *Advances in theoretical hydrology - a tribute to James Dooge*. Elsevier Science, Amsterdam, pp 129-157.

Griesbach, I., 2004. Validierung modellierter kontinentaler Wassertransporte, TU-Dresden, Institut für Planetare Geodäsie - Astronomie, 2004.

Hagemann, S., Dümenil, L., 1998. A parametrization of the lateral waterflow for the global scale. *Climate Dynamics* **14**, pp. 17-31, Springer Verlag 1998.

Hagemann, S., Dümenil, L., 1998. Documentation for the Hydrological Discharge Model, *Technical Report* No. **17**. Max Planck Institute for Meteorology, Hamburg, Germany.

Hagemann, S., Dümenil Gates, L., 2003. Improving a subgrid runoff parameterization scheme for climate models by the use of high resolution data derived from satellite observations. *Clim. Dyn.* **21**, pp. 349-359.

Mintz, Y., Walker, G.K., 1993. Global Fields of Soil Moisture and Land Surface Evapotranspiration Derived from Observed Precipitation and Surface Air Temperature. *J. Applied. Meteor.* **32**, pp. 1305-1334.

Mitsch, W.J., Gosselink, J.G., 1993. Wetlands. Second edition. Van Nostrand Reinhold, New York.

Oki, T., Nishimura, T., Dirmeyer, P., 1999. Assessment of annual runoff from land surface models using Total Integrated Pathways (TRIP). *J. Meteor. Soc. Japan* **77**, pp. 235-255.

Roeckner, E., Arpe, K., Bengtsson, L., Brinktop, S., Dmenil, L., Esch, M., Kirk, E., Lunkeit, F., Ponater, M., Rockel, B., Sausen, R., Schlese, U., Schubert, S., Windelband, M., 1992. Simulation of the present-day climate with the ECHAM model: impact of model physics and resolution. *Max-Planck-Institute for Meteorology Rep* **93**, Hamburg.

Schmitz-Hübsch, H., Dill, R., 2001. Atmospheric, oceanic and hydrological influences on Earth rotation. *ZfV* **5/2001**.

Singh, V.P., 1988. Rainfall-runoff modelling. *Hydrologic systems* vol. **1**. Prentice Hall.

Sündermann et al., 2008. Physically consistent system model for the study of the Earth's rotation, surface deformation and gravity field parameters. *DFG series C*, in preparation.

Van Hylckama, T.E.A., 1970. Water Balance and Earth Unbalance. *Int. Ass. of Scientific Hydrology Publication* No. **93**, Symp. on World Water Balance, vol. 2, pp. 434-444.

Vörösmarty, C.J., Fekete, B.M., Meybeck, M., Lammers, R., 2000. Geomorphometric attributes of the global system of rivers at 30-minute spatial resolution. *J. Hydrology* **237**, pp. 17-39.

Wahr, J.M., 1983. The effects of the atmosphere and oceans on the Earth's wobble and on the seasonal variations in the length of day-II. Results, *Geophys. J. Roy. astr. Soc.* **74**, pp. 451-487.

Walter, C., 2008. Simulation hydrologischer Massenvariationen und deren Einfluss auf die Erdrotation. Phd-thesis, TU Dresden, Germany.

Wigmosta M.S., Vail L., Lettenmaier, D.P., 1994. A distributed hydrology-vegetation model for complex terrain. *Water Resource Res.* **30**, pp. 1665-1679.

STR08/09

Robert Dill, Hydrological model LSDM

ISSN 1610-0956